General model for explicitly hole-doped superconductor parent compounds: Electronic structure of $Ca_{2-x}Na_xCuO_2Cl_2$ as a case study

Pablo Rivero,[1] Ibério de P. R. Moreira,[1] Ricardo Grau-Crespo,[2] Sambhu N. Datta,[3] and Francesc Illas[1,*]

[1]*Departament de Química Física & Institut de Química Teòrica i Computacional (IQTCUB), Universitat de Barcelona, C/Martí i Franquès 1, E-08028 Barcelona, Spain*

[2]*Department of Chemistry, University College London, 20 Gordon Street London WC1H 0AJ, United Kingdom*

[3]*Department of Chemistry, Indian Institute of Technology, Bombay, Powai, Mumbai-400076, India*

(Received 6 May 2013; revised manuscript received 19 June 2013; published 7 August 2013)

Periodic density functional theory (DFT) + U calculations using sufficiently large supercells to explicitly account for dopant disorder are reported for undoped $Ca_2CuO_2Cl_2$ and for the doped $Ca_{2-x}Na_xCuO_2Cl_2$ ($x = 0.125$ and $x = 0.250$). For the undoped material, the charge-transfer antiferromagnetic character is properly reproduced. For the doped systems, a metallic character is predicted with the conduction band dominated by the O(2p) states, with doping having a small effect on the antiferromagnetic order of the Cu^{2+} cations within the CuO_2 planes while maintaining the diamagnetic character in the rest of centers. The analysis of the spin density plots for the doped material evidences the appearance of a new feature reminiscent of the so-called Zhang-Rice singlet, thus providing unbiased independent support to the corresponding model Hamiltonian. However, it is also worth pointing out that the present DFT picture provides only an average static representation of what is expected to be a dynamic electronic structure.

DOI: 10.1103/PhysRevB.88.085108 PACS number(s): 31.15.E−, 74.20.Pq, 71.23.−k

I. INTRODUCTION

Nearly 30 years after the discovery of superconductivity in ceramic Cu-containing compounds by Bednorz and Müller,[1] a general theory explaining this surprising physics is still missing. In part, the difficulty arises from the nonstoichiometric character of these cuprates, which exhibit superconductivity only after appropriate doping.[2,3] The hole or electron doping transforms the material from insulator to superconductor but only for a small concentration of dopants in a very specific range. The optimal doping for a given cuprate is defined as the one for which the critical temperature (T_c) is the highest. For instance, La substitution by Sr in La_2CuO_4 results in nonstoichiometric $La_{2-x}Sr_xCuO_4$, which achieves the maximum T_c of 39 K for $x = 0.15$,[4] and Ca substitution by Na in $Ca_2CuO_2Cl_2$ results in $Ca_{2-x}Na_xCuO_2Cl_2$ with a maximum $T_c = 26$ K also for $x = 0.15$ (see Ref. 5). Hole doping can also be achieved by excess of oxygen or fluorine atoms in interstitial sites as in $La_2CuO_{4+\delta}$, $Sr_2CuO_2F_{2+\delta}$ ($T_c = 46$ K for $\delta \sim 0.6$) or $HgBa_2CuO_{4+\delta}$ ($T_c = 97$ K for $\delta = 0.09$), the latter holding the highest T_c value observed so far for single-layered cuprates.[6] In all cases, atomic substitutions are localized out of the CuO_2 planes. Nevertheless, these substitutions have an indirect effect over the effective charge in the CuO_2 planes,[7,8] leading to the superconductor phase.

The electronic structure of the undoped compounds has been a matter of controversy since earlier theoretical studies based on the local density approach (LDA) of density functional theory (DFT) predicted these materials to have a metallic character.[4] This exciting prediction was, however, proven wrong, as accurate experiments undoubtedly revealed that the stoichiometric materials are antiferromagnetic (AFM) insulators.[2,3] The AFM character of these compounds was properly predicted by calculations using embedded cluster models to represent the materials and explicitly correlated configuration interaction wave functions.[9,10] This type of approach was able even to quantitatively reproduce the magnitude of the magnetic coupling constant, a rather elusive property, in a rather large series of undoped cuprates.[11,12] However, one could still argue that the periodic nature of the materials was not properly taken into account in these studies. The study of Muñoz *et al.*[13] using the Hartree-Fock method and either a periodic approach or an embedded cluster model to represent the material has proven that the cluster model representation does not introduce any bias in the description of the prediction of the magnetic coupling of these materials. Subsequent studies based on DFT methods that go well beyond the LDA formalism have reconciled theory and experiment and properly predicted not only the AFM character of these compounds but again accurately reproduced the magnitude of the magnetic coupling constant regardless of whether a cluster[14] or a periodic model[15] is used to represent the undoped cuprates. Therefore, one can affirm that the electronic structure of the stoichiometric cuprates, often referred to as superconducting parent compounds, is now almost completely understood. However, the fact remains that superconductivity only emerges after doping the material with either electrons or holes.[2,3]

Clearly, to approach the electronic structure of the superconducting materials, it is necessary to explicitly consider doping in some way. Earlier approaches employed model Hamiltonians with parameters taken from either experiment or from theoretical calculations. In the first case, one needs to use experimentally measured properties such as electronic transitions to assign values to the parameters of the model Hamiltonian, which in this way loses predictive power. The second approach is not free of problems since we have already commented that an accurate description of the electronic structure has been difficult to achieve even for the parent compounds. Nevertheless, these approximate theoretical descriptions have been extremely important and exposed a

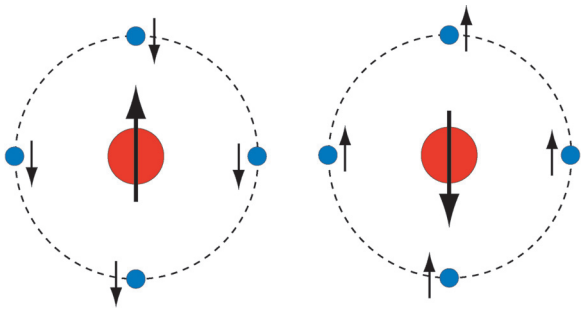

FIG. 1. (Color online) Schematic representation of the two possible situations of Zhang-Rice (open-shell) singlets. Note that the spin density on the O atoms (blue) is 1/4 of the corresponding value on the Cu site (red) to indicate the dynamic character of this entity. Note also that a proper description of each singlet requires the appropriate spin combination.

large amount of the essential physics and many important concepts. This is the case of the so-called Zhang-Rice singlet,[16] which aims at providing a first explanation of the disappearance of AFM coupling upon doping by holes. In this model, one electron is removed from the O(2p) band and the resulting hole couples to the unpaired electron of the Cu^{2+} cation thereby forming a local singlet with a concomitant quenching of the total magnetic moment of the doped material, as schematically shown in Fig. 1. The coupling is, however, dynamic and involves simultaneously several instantaneous electron distributions. This is because this is a purely many-electron effect, and its proper description requires using a superposition of states, or a configuration interaction-type wave function. In this way, the four O atoms surrounding each Cu^{2+} cation in a CuO_4 unit of the CuO_2 planes are all instantaneously involved. The simple Zhang-Rice singlet picture[16] emerges from the so-called t-J model Hamiltonian initially proposed by Anderson.[17] This is essentially a one-band model that simultaneously takes into account the AFM interactions between the magnetic moments localized at the Cu sites and the presence of holes in the Cu-O planes and can be regarded as a simplification of the three-band Hubbard model Hamiltonian of Emery[18] that implicitly includes the O(p)-Cu(d) hybridization.

In order to include the effect of the dopant and to provide an explanation of the dependence of T_c on the composition of the material, several different ideas have been discussed. The latter involves charge-ordering effects,[19] band-structure variations,[20] dopant-induced disorder,[21] and several other phenomena. Nevertheless, despite intense research on the mechanism of superconductivity in this kind of materials, not much is known yet about the details of how the electron or hole is created within the CuO_2 plane. Clearly, a more elaborate description of the electronic structure of the doped cuprates requires the doping to be explicitly included in the model, which for realistic concentrations of the dopant implies using very large supercells, thus requiring a computational effort that has become possible only very recently.[22–24] Anisimov *et al.*[22] reported a DFT-based study of $La_{1.88}Sr_{0.12}CuO_4$ in which the LDA + U exchange-correlation potential[25–27] is used to avoid the unphysical description of the Cu(3d) orbitals provided by LDA. The empirical U term penalizes double occupancy; this favors spin localization and provides the correct AFM charge-transfer electronic ground state. A somewhat better description has been provided by Patterson, who employed the hybrid B3LYP exchange-correlation potential,[28,29] including a part of the nonlocal Fock exchange, to study $Ca_{2-x}Na_xCuO_2Cl_2$. The amount of Fock exchange comes from fitting to experiment thermochemical data for a large set of molecular systems, and, therefore, the procedure is not exempt from some amount of empiricism. LDA + U and B3LYP differ, however, in that in the former, only the Cu(3d) band is corrected, whereas in the latter, all the one-electron states are affected by the nonlocal Fock exchange. Cluster models and quantum chemical methods have also been used to study the effect of hole doping in the local electronic structure, although the limitations of the model here are more important than in the case of undoped materials; the results herein are difficult to compare with the experimental situation.[30]

In spite of the progress achieved by the pioneering work of Anisimov *et al.*[22] and Patterson,[24] several issues still require clarification and further work. A possible weakness in the model used by Anisimov *et al.*[22] is the use of a stoichiometric unit cell where the charge injection by the dopant is artificially introduced in the model and compensated by a uniform background charge density of opposite sign. This charge-compensating model has also been used by Patterson,[24] although the latter author employs large supercells representing the nonstoichiometric-doped cuprates. In order to carry out the calculations involving these large supercells, Patterson made an assumption regarding the symmetry of the supercell, namely, that the dopant atom per unit cell is symmetrically replicated and thus not adequately representing the disordered nature of the doped phases. In the present work, an attempt is made to go one step beyond these previous studies[22,24] and explicitly consider the effect of dopants and their disorder on the electronic structure of the cuprate. To this end, we will focus on Na-doped $Ca_2CuO_2Cl_2$, where a fraction of Ca atoms has been replaced by Na leading to a $Ca_{2-x}Na_xCuO_2Cl_2$ formula unit while considering large enough supercells and taking into account all symmetrically unique ionic configurations for any particular composition. The choice of this material comes from the fact that it is one of the most experimentally studied doped cuprates: it has been extensively studied using photoemission experiments,[31,32] and the inhomogeneous character of the electronic structure has been explored by scanning tunneling microscopy.[33–38] Moreover, the undoped system exhibits a simple crystal structure, which facilitates the calculations. It has been shown that upon doping, Cooper pairs in the CuO_2 planes involving holes rather than electrons are formed in this material, with the resulting phase exhibiting superconductor character, and T_c reaching a maximum of 26 K at an optimal doping of $x = 0.10$.[39]

This paper is organized as follows. Section II describes the models used to study the Na doping of $Ca_2CuO_2Cl_2$ with explicit consideration of the dopants and their distribution. Section III describes the settings and approximations for our quantum-mechanical calculations. Section IV presents and discusses our theoretical results. Finally, in Sec. V, our conclusions are given.

II. SUPERCELL MODELS FOR Na-doped $Ca_2CuO_2Cl_2$

To study the electronic structure of the $Ca_{2-x}Na_xCuO_2Cl_2$-doped system by means of a periodic model, it is necessary to start from the crystal structure of the undoped $Ca_2CuO_2Cl_2$ system. This material exhibits a tetragonal $I4/mmm$[40] structure at all temperatures below the melting point, and its cell parameters are $a = b = 3.869$ Å and $c = 15.05$ Å with atoms located at Cu(0,0,0), O(1/2, 0, 0), Ca (0,0,0.396), and Cl (0,0,0.183) fractional coordinates in the crystal unit cell. This cuprate has been found to be a charge-transfer AFM insulator with a Néel temperature of 250 K.[41,42] Note that, similar to most cuprates, this structure involves CuO_2 planes well separated by counterion planes, including Ca and Cl ions stacked along the c crystallographic axis (Fig. 2).

Explicit doping using a periodic model requires the use of a supercell and the substitution of one or more Ca^{2+} cations by Na^+ cations, which, to maintain electroneutrality, introduces one hole per Na^+ in the CuO_2 planes of the supercell. Note, however, that the overall electronic structure is subsequently variationally relaxed, and, hence, this way of reasoning does not introduce any bias in the model. In this paper, we consider models representing two different dopant concentrations, namely $x = 0.125$ and $x = 0.250$. The case for $x = 0.125$ has already been considered by Patterson[24] in a supercell model, including a single substitution and imposing a symmetry constraint in the c direction. In this paper, we use a similar model but without any symmetry constraint, which implies considering larger supercells. In addition, the case with $x = 0.250$ implies more substitutions per unit cell and, consequently, a larger number of possible distributions of Na cations in the unit cell. In this way, the latter allows us to explicitly consider the effect of the dopant distribution on the stability and on the electronic structure of the doped system, which has not been taken into account in previous investigations.

For $x = 0.125$, we choose a supercell that corresponds to a $2 \times 2 \times 1$ multiple of the conventional unit cell shown in Fig. 2.

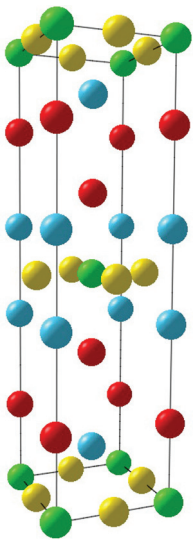

FIG. 2. (Color online) The unit cell of the $Ca_2CuO_2Cl_2$ cuprate. Green, yellow, red, and light blue correspond to Cu, O, Cl, and Ca, respectively.

For the undoped system, this would lead to a $Ca_{16}Cu_8O_{16}Cl_{16}$ supercell. By substituting one Ca atom by one Na atom, one gets $Ca_{15}Na_1Cu_8O_{16}Cl_{16}$, and, in this way, a hole state is introduced, which, in principle, is localized in one of the CuO_2 layers in the supercell. There are 16 Ca sites in the supercell where Na can be substituted, but all of them are symmetrically equivalent. In the following discussion, we refer to the unique configuration with this composition as Q1. Clearly, this model allows one to study the effect of introducing one hole in the electronic structure but does not permit us to scrutinize the effect of disorder of the dopant. To explicitly consider disorder, we still use the $2 \times 2 \times 1$ supercell but with two Ca substituted by two Na, leading to $Ca_{14}Na_2Cu_8O_{16}Cl_{16}$ or, equivalently, $Ca_{1.75}Na_{0.25}CuO_2Cl_2$. For this supercell and composition, a symmetry analysis by the SOD code[43] reveals that there are seven possible nonequivalent configurations, which have all been explicitly considered in this work. The nonequivalent configurations for the overdoped cuprate will be referred to as Q2-1, Q2-2, . . . , Q2-7, respectively.

III. COMPUTATIONAL DETAILS

The electronic structures of the undoped $Ca_2CuO_2Cl_2$ cuprate and of the $Ca_{15}Na_1Cu_8O_{16}Cl_{16}$ and $Ca_{14}Na_2Cu_8O_{16}Cl_{16}$ models of $Ca_{2-x}Na_xCuO_2Cl_2$ for $x = 0.125$ and 0.250 doped systems have been studied by means of periodic DFT-based calculations carried out with a plane-wave basis set and the projected augmented wave (PAW) description of the atomic cores.[44,45] The simple LDA exchange correlation potential with the on-site Coulomb U correction has been employed.[25–27] The resulting LDA + U scheme represents a good compromise between accuracy and computational cost to provide a physically meaningful description of strongly correlated solids. A value of 8 eV has been chosen for the U parameter, which has been shown to provide a reasonable description of the band gap and magnetic coupling in a rather large group of monolayered cuprates, $Ca_2CuO_2Cl_2$ among them.[46] In all cases, the crystal structures have been optimized employing a conjugate gradient algorithm[47]; both cell parameters and atomic positions have been fully relaxed.

For the LDA + U calculations on the supercells described in the previous sections, the PAW chosen are such that they leave Cu with 17 valence electrons ($3p^6$, $3d^{10}$, $4s^1$), O with 6 ($2s^2$, $2p^4$), Cl with 7 ($3s^2$, $3p^5$), and Ca with 8 ($3p^6$, $4s^2$). The quality of the plane-wave basis set is controlled by kinetic energy cutoff that determines the number of plane waves included in the calculation. In this paper, we have used a high value of 650 eV (50% above the standard value for the potentials employed), which is necessary to accurately describe the energy difference between configurations. A $4 \times 4 \times 2$ Monkhorst-Pack grid special k-point has been used to carry out the numerical integration in the reciprocal space.

Before closing this section, it is important to describe the different magnetic solutions that one can obtain for each one of the supercells considered for the undoped and doped materials. In the case of the undoped materials, it is sufficient to consider one unpaired electron per Cu^{2+} center in a $d_{x^2-y^2}$ magnetic orbital, which gives rise to the well-known ferromagnetic (FM) and AFM solutions,[9–15] the latter being the ground state

in all known cuprates.[4] Note that in these solutions the z component of the total spin (S_z) for the (double) supercell is either 1 or 0. However, in the doped materials, different new possibilities emerge depending on the total S_z resulting from the coupling with the additional unpaired electrons introduced by Na substitutions in the undoped cuprate. In the case of $x = 0.125$, the supercell contains eight Cu^{2+} cations. It is possible to obtain three different magnetic solutions, namely (i) AFM ordering of the magnetic moments in the Cu^{2+} cations, with one additional unpaired electron resulting in a total $S_z = 1/2$; and (ii) and (iii) FM ordering of the magnetic moments in the eight Cu^{2+} cations, with one additional unpaired electron either with spin up or spin down, resulting in a total $S_z = 9/2$ and $S_z = 7/2$. In the case of heavier doping ($x = 0.250$), one still has eight Cu^{2+} cations but needs to consider two holes or, in other words, two new unpaired electrons per unit cell, giving rise to four different magnetic solutions: (i) AFM ordering of the magnetic moments in the Cu^{2+} cations, with two additional unpaired electrons FM or AFM coupled, resulting in a total $S_z = 1$ or $S_z = 0$; and (ii) FM ordering of the magnetic moments in the Cu^{2+} cations, with two additional unpaired electrons FM or AFM coupled, resulting in a total $S_z = 5$ or 4. The magnetic solutions described correspond to the simplest ones because they maintain the FM or AFM order in the CuO_2 plane. Other solutions exist with intermediate spin ordering in the CuO_2 plane defining the spectrum of magnetic excitations for this supercell. In the case of doped systems, these intermediate states are not relevant because the final energy is dominated by the coupling with the new unpaired electrons.

All calculations in this work have been carried out with the Vienna *ab initio* Simulation Package.[48,49]

IV. RESULTS AND DISCUSSION

The electronic structure of the undoped $Ca_2CuO_2Cl_2$ parent compound was studied in detail by means of different DFT-based methods, including LDA + U and hybrid exchange-correlation potentials.[15,24,50] Therefore, the results corresponding to the undoped compound will not be discussed here. We only mention that the two approaches properly predict the compound to be an AFM insulator and also quantitatively reproduce the measured band gap. Moreover, calculated values of the magnetic coupling constants for the $Ca_2CuO_2Cl_2$ parent compound are in line with those corresponding to similar systems for which results from cluster-model configuration-interaction calculation or the experimental data exist.[11–13] Here, let us recall that the calculated values for the parent compound are $J = -143$ meV using LDA + U (U = 8 eV) and $J = -198$ meV using B3LYP, while the experimental value is still unknown. It is also important to point out that while LDA + U remedies most of the deficiencies of LDA, it still fails to properly describe the charge-transfer nature of the electronic band gap of this type of compound, especially for La_2CuO_4. Nevertheless, it is expected that LDA + U will be adequate to provide a reasonable description of the electronic structure of $Ca_2CuO_2Cl_2$ and the hole-doped systems. The comparison below between our results and those reported by Patterson[24] for the small unit cell using the hybrid B3LYP functional strongly supports this hypothesis.

We first consider the case of $x = 0.125$ corresponding to the Q1 ($2 \times 2 \times 1$) supercell and involving the substitution of one Ca atom by Na; this is exactly the system previously studied by Patterson.[24] We already mentioned that among the possible Ca positions for Na substitution, a simple symmetry analysis reveals that there is only one nonequivalent configuration of the doped supercell. Figure 3 display the density of states (DOS) plot corresponding to the AFM CuO_2 planes with an additional hole ($S_z = 1/2$) solution (left panel) and that of the AFM ground state of the undoped system as obtained from a double cell to allow for AFM order (right panel). In agreement with the periodic B3LYP calculation of Patterson,[24] the DOS plot for the doped supercell shows a metallic solution. The origin of the metallic solution provoked by Ca substitution by Na is a shift of the valence band of the undoped compound toward higher energies, crossing the Fermi level and thus becoming the conduction band. Figure 3 also evidences a small contribution of the spin polarization caused by the presence of one electron hole in the supercell, which contrasts with the common assumption that doping induces a constant (rigid) shift of all bands.

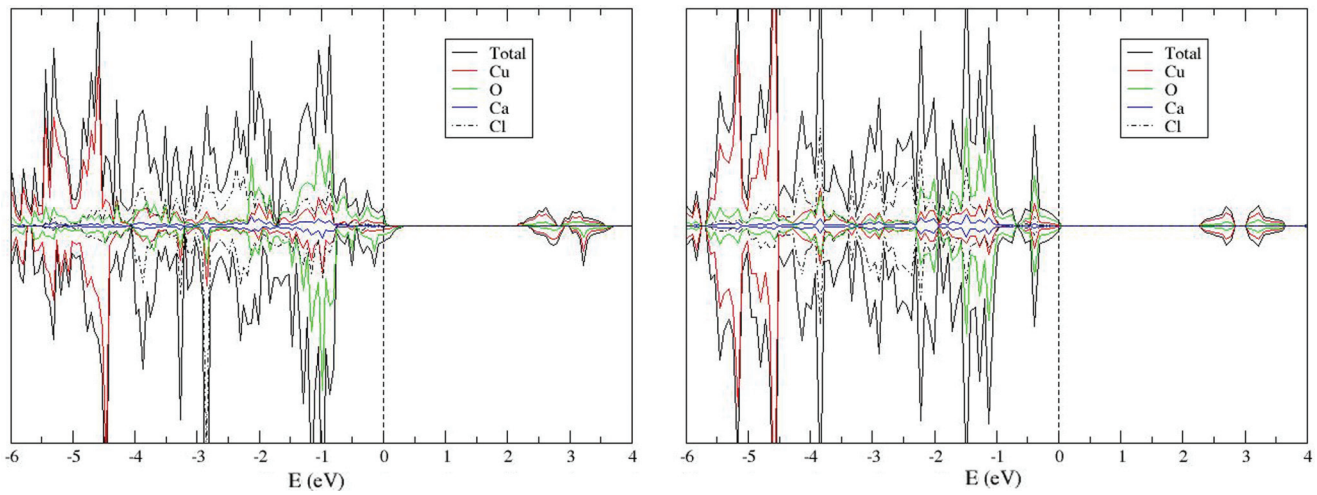

FIG. 3. (Color online) Density of states of the ground state of Na-doped ($x = 0.125$) and undoped $Ca_2CuO_2Cl_2$ cuprate, as obtained from LDA + U calculations on the Q1 ($Ca_{15}Na_1Cu_8O_{16}Cl_{16}$; left panel) and double ($Ca_4Cu_2O_4Cl_4$; right panel) supercells, respectively.

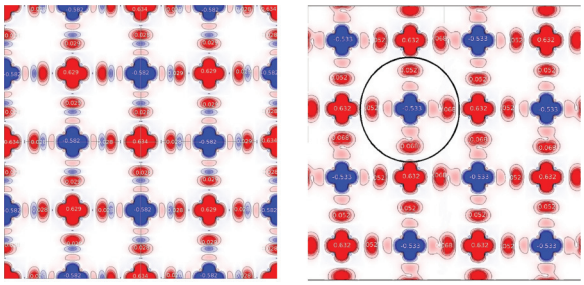

FIG. 4. (Color online) Spin density maps for $z = 0$ (left) and $z = 0.5$ (right) crystallographic planes (cf. Fig. 1) of the doped Q1 ($Ca_{15}Na_1Cu_8O_{16}Cl_{16}$) phase of $Ca_{1.875}Na_{0.125}CuO_2Cl_2$. The circle in the right panel evidences a feature attributable to a Zhang- Rice type singlet. The separation between isolines is 0.05 e/Bohr^3.

To better understand the effect of the Na dopant in the electronic structure of $Ca_2CuO_2Cl_2$, we present in Fig. 4 spin density maps for the basal (left panel) and central CuO_2 planes, the latter being closer to the plane containing the (periodically repeated) Na substitutions. The spin density map in the left panel is indistinguishable from the one corresponding to the undoped material (not shown), whereas the map in the right panel, explained in detail below, evidences a new feature that is reminiscent of the Zhang-Rice singlet,[16–18] thus indicating that the corresponding model Hamiltonian has the right physics or at least has a physics that coincides with this LDA + U description of the electronic structure. Here, one must point out that the correct description of the Zhang-Rice singlet implies a superposition of states and, therefore, requires a many-electron wave function to be properly described. It is not possible to rigorously claim that the present approach evidences the existence of the Zhang-Rice singlet, precisely because of the one-electron average description of electron correlation in DFT-based methods. With all these caveats, it is still possible to suggest that the spin density maps in Fig. 4 correspond to an averaged picture of this dynamic many-electron entity. We note that a similar interpretation of this feature has been reported in the elegant work of Patterson. It is important to mention that in spite of representing the same dopant concentration, the supercell used in the present work for Q1 is different from that used by Patterson. This is because Patterson employed a larger supercell to accommodate a larger number of CuO_2 units per supercell plane and, in turn, had to force a higher (P_m) symmetry, implying equivalence of CaCl planes in pairs so that substitution necessarily affects planes above and below the central plane. The use of a higher symmetry by Patterson resulted in a strongly localized effect, which was interpreted as a spin polaron. On the contrary, in this paper the Na dopant is only introduced in one of the possible planes thus allowing for a differential effect between the doped and undoped CaCl planes, and the possible spin polaron resulting from the optimized crystal structure is not as localized. Note also that Patterson uses a hybrid B3LYP-like DFT approach, whereas the DFT + U scheme is used here. Both approaches have some arbitrariness, and the difference degree of polaronic distortion is not totally unexpected. In any case, the most relevant point is that present calculations confirm the findings of Patterson and show that the appearance of the Zhang-Rice singlet features in his calculations is not induced by imposing a higher symmetry. One can argue that the present Q1 model represents an artificially ordered doping situation around a given CuO_2 plane. The calculations for the Q2 phases discussed below introduce disorder explicitly in the supercell and, hence, show that results in Fig. 4 are not an artifact of a particular ordering of the dopants.

TABLE I. Spin density population on Cu and O sites based on Bader analysis for undoped ($x = 0$) and several doped phases of $Ca_{2-x}Na_xCuO_2Cl_2$ (see text).

x	Phase	μ (Cu↑)	μ (Cu↓)	μ (O↑)
0	AFM	+0.63	−0.63	0.00
0.125	Q1	+0.63	−0.53/−0.58	0.03/0.07
0.250	Q2-1	+0.64	−0.45	0.07
0.250	Q2-2	+0.64	−0.45	0.07

Before describing the Q2 phases in more detail, it is important to point out that while the presence of the dopant introduces a local point defect in the atomic structure, it also affects the whole electronic structure of the CuO_2 plane. Thus, all spin-up Cu^{2+} cation in the doped system experience a reduction on their spin density by (open-shell singlet) coupling to the antiparallel spin density in all O anions in that plane arising from the hole injection. Note also that the spin density of the spin-down Cu^{2+} cations, however, remains unchanged as in the undoped system. This is clear from the comparison of spin density values for undoped and Q1 phases in the first and second rows of Table I. This picture implies that the physics of the Zhang-Rice singlet is more complex than imagined from a simple scheme as in Fig. 1. The coupling between the (down) spin density in the O(2p) band introduced by the hole injection affects the (up) spin density of half of the cations in the CuO_2 plane. While the effective model Hamiltonian[16–18] leading to the Zhang-Rice singlet implies that the coupling is dynamic, however, the present DFT picture provides only an average static representation. This is why taking into account strong correlation effects explicitly is necessary to describe the fluctuations governing the low-temperature physics. In any

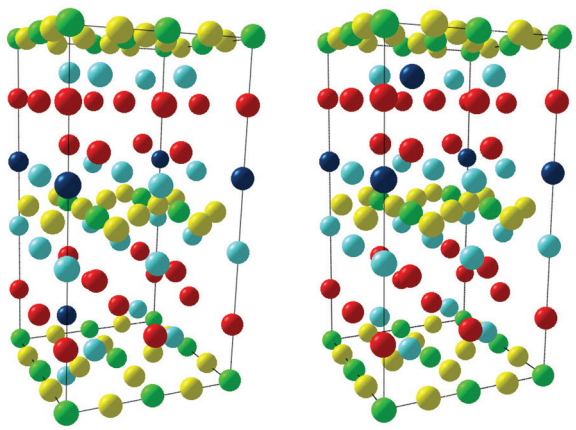

FIG. 5. (Color online) The Q2-1 (left) and Q2-2 (right) configurations corresponding to the most stable situation for a double substitution of Ca by Na in the $Ca_{16}Cu_8O_{16}Cl_{16}$ supercell. Green, yellow, red, light blue, and dark blue correspond to Cu, O, Cl, Ca, and Na, respectively.

TABLE II. Relative energies of the Q2 unique configurations of $Ca_{2-x}Na_xCuO_2Cl_2$ ($x = 0.250$) in meV per Cu atom (8 Cu atoms in Q2 supercells) relative to the most stable one.

Configuration	ΔE (meV)
Q2-1	0
Q2-2	0.003
Q2-3	0.078
Q2-4	0.101
Q2-5	0.142
Q2-6	0.155
Q2-7	0.251
Q2-FM	2.160

case, the observation that the present DFT calculations support the model based on the presence of Zhang-Rice entities is already extremely appealing, although one must also admit that, in part, this is biased because of the inherent mean-field nature of DFT-based methods.

The relative stability of the Q2 phases, containing two dopants in the unit cell simultaneously, is reported in Table I; the most stable situations, corresponding to Q2-1 and Q2-2 configurations, are displayed in Fig. 5. We have already commented that substitution of two Ca by two Na atoms on the $Ca_{14}Na_2Cu_8O_{16}Cl_{16}$ unit leads to seven different (symmetrically nonequivalent) configurations. Obviously, the total energy corresponding to the fully optimized structure of each of these configurations is different and provides a measure of the probability of finding them in a real sample. Introduction of the dopant slightly modifies the lattice parameters with a very small contraction of the cell volume and a small modification of the atomic positions near the dopant, as expected from the very similar ionic radius of Ca^{2+} and Na^{+} cations. An identical situation is found for the Q1 phase, although this has not been commented before. For these Q2-1 and Q2-2 cases, the total energy per Cu atom differs by 3 meV only, whereas the next most stable configuration (Q2-3) is significantly less stable (78 meV per Cu higher in energy than Q2-1). The relative energies all Q2 configurations are reported in Table II. It is interesting to mention that the most stable situations correspond to cases where the distance between the two Na centers is the longest possible, and substitution occurs in different planes in the cell, leading to the maximum possible homogeneity in the dopant distribution. Notice that this preferential distribution is not respected in the model of Patterson where, because of the use of the P_m space group to reduce the computational burden, the distribution of Na cations is constrained by symmetry. The present results for the Q2 phases thus indicate that the distribution of disorder among the dopants has to be explicitly accounted for, which requires considering different cation configurations in a sufficiently large unit cell.

Figure 6 displays the DOS for the Q2-1 and Q2-2 phases in their electronic ground state, which corresponds to a high-spin coupling of the unpaired electrons injected in the O(2p) band while maintaining the AFM coupling between the eight Cu^{2+} cations in the supercell. It is also important to point out that the solution forcing $S_z = 0$ in the unit cell lies at a 115 meV higher energy, which provides an estimate of the cost to break down the Zhang-Rice singlet local entities. The analysis of Fig. 6 reveals similarities with Fig. 3 corresponding to $x = 0.125$. Both doped systems are metallic, and the higher dopant concentration in the Q2 supercells ($x = 0.250$) results in a more intense peak at the Fermi level, which suggests a better metallic conductivity. Unfortunately, this static picture of the electronic structure does not permit us to extract any information about the superconductivity below T_c in the doped system, but it does allow us to explain the metallic character at temperatures above T_c. This is not a trivial conclusion since the undoped system is a charge-transfer AFM insulator, a character properly reproduced by the present DFT + U approach.

Finally, Fig. 7 displays the spin density plots for the two different planes of this cuprate, as obtained from Q2-1 electron ground state; an identical plot is obtained for the near degenerate Q2-2 situation. These spin plots confirm the picture discussed for the lower doping concentration ($x = 0.125$), although in the Q2-1 phase there larger differences in the spin density at the Cu centers, and the spin density at O centers is also larger than the one corresponding to the Q1

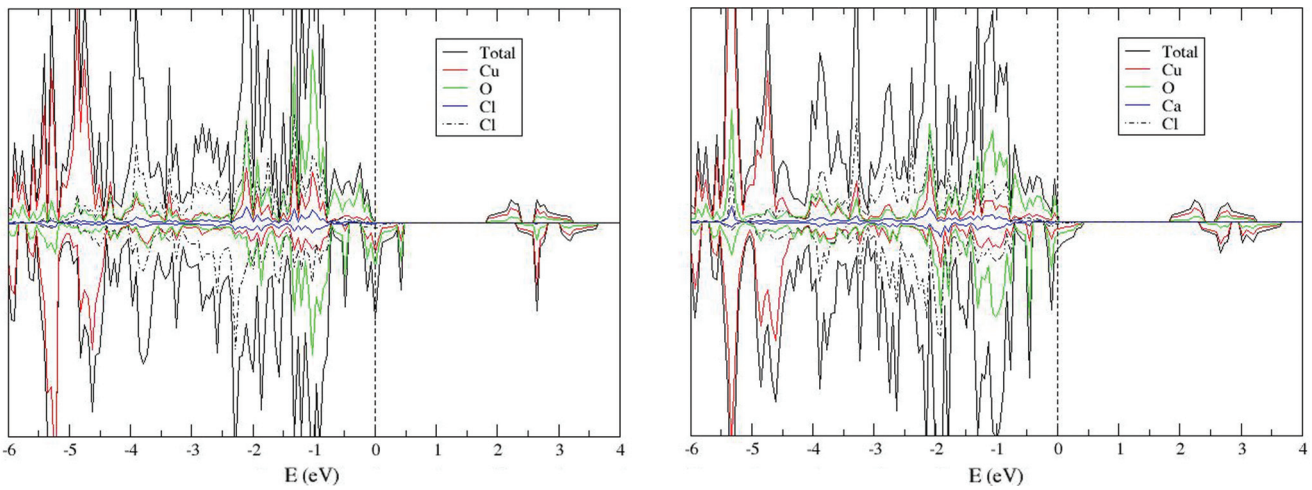

FIG. 6. (Color online) Density of states of the ground state of Na-doped ($x = 0.250$) and undoped $Ca_2CuO_2Cl_2$ cuprate, as obtained from LDA + U calculations on the Q2-1 (left) and Q2-2(right) supercells.

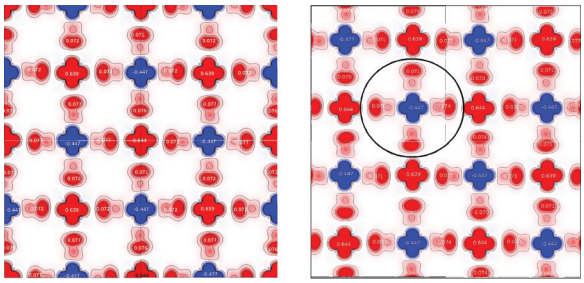

FIG. 7. (Color online) Spin density maps for $z = 0$ (left) and $z = 0.5$ (right) crystallographic planes (cf. Fig. 1) of the doped Q2-1 ($Ca_{14}Na_2Cu_8O_{16}Cl_{16}$) phase of $Ca_{1.750}Na_{0.250}CuO_2Cl_2$. Similar to the case for $x = 0.125$ in FIG. 4, the circle in the right panel evidences a feature attributable to a Zhang-Rice type singlet. The separation between isolines is 0.05 e/Bohr^3.

case. Hence, the present results allow one to firmly claim that the type of Zhang-Rice entity appearing either in Figs. 4 or 7 are not artifacts from the model used to study the doped system but correspond to a genuine physically meaningful picture.

V. CONCLUDING REMARKS

In this paper, a first-principle based picture is given for the undoped $Ca_2CuO_2Cl_2$ cuprate and for the phases corresponding to close to optimal ($x = 0.125$) and overdoped ($x = 0.250$) $Ca_{2-x}Na_xCuO_2Cl_2$ material based on periodic LDA + U calculations. The situation with $x = 0.125$ has been represented by a $Ca_{15}Na_1Cu_8O_{16}Cl_{16}$ supercell, where, due to symmetry, there is only one possible way to substitute Ca by Na. In the $x = 0.250$ case, seven distinct symmetry situations are possible for the $Ca_{14}Na_2Cu_8O_{16}Cl_{16}$ supercell, thus allowing the consideration of disorder effects in the doped systems. All these configurations were explicitly calculated in order to understand the preferential distribution of the dopants, which are not symmetry related in the real doped material.

For the undoped material, the experimentally found charge-transfer AFM character is properly reproduced. For the doped systems, the DOS reveals a metallic character with the conduction band dominated by the O(2p) states, as expected in the case of hole doping. Moreover, the metallic character is enhanced when increasing the dopant concentration. However, introduction of holes in the O(2p) band has a small effect on the AFM order within the Cu^{2+} cations in the CuO_2 planes and maintains the diamagnetic character in the rest of the centers.

The analysis of the spin density plots shows that for the two doping concentrations, a new feature emerges that is reminiscent of the Zhang-Rice singlet.[16–18] Hence, the corresponding model Hamiltonian leads to a description that agrees with the one obtained from unbiased electronic structure calculations. Consequently, it is possible to claim that this model Hamiltonian contains a significant amount of the right physics. However, it is also worth pointing out that while the effective model Hamiltonian[16–18] leading to the Zhang-Rice singlet implies that the coupling is dynamic, the present DFT picture provides only an average static image, although it already offers an explanation for the metallic character at temperatures above T_c.

ACKNOWLEDGMENTS

This work has been supported by Indo-Spain Collaborative Program in Science—Nanotechnology (DST Grant No. INT-Spain-P42-2012 and Spanish Grant No. PRI-PIBIN-2011-1028); Spanish MICINN and MINECO research Grants No. FIS2008-02238 and No. CTQ2012-30751; and, in part, by *Generalitat de Catalunya* Grants No. 2009SGR1041 and No. XRQTC. P.R. thanks Spanish MICINN for a predoctoral grant; F.I. acknowledges additional support from the 2009 ICREA Academia award for excellence in research; and S.N.D. is grateful to DST Grant No. SR-S1-PC-19-2010 for financial support of this work.

*Corresponding author: francesc.illas@ub.edu

[1] J. G. Bednorz and K. A. Müller, Z. Phys. B **64**, 189 (1986).
[2] M. R. Norman and C. Pepin, Rep. Prog. Phys. **66**, 1547 (2003).
[3] A. Damascelli, Z. Hussain, and Zhi-Xun Shen, Rev. Mod. Phys. **75**, 473 (2003).
[4] E. Dagotto, Rev. Mod. Phys. **66**, 763 (1994).
[5] Z. Hiroi, N. Kobayasi, and M. Takano, Physica B **266**, 191 (2006).
[6] J. L. Wagner, P. G. Radaelli, D. G. Hinks, J. D. Jorgensen, J. F. Mitchell, B. Dabrowski, G. S. Knapp, and M. A. Beno, Physica C **210**, 447 (1993).
[7] C. Ambrosch-Draxl, P. Süle, H. Auer, and E. Y. Sherman, Phys. Rev. B **67**, 100505 (2003).
[8] P. Dore, G. De Marzi, R. Bertini, A. Nucara, P. Calvani, and M. Ferretti, Physica C **350**, 55 (2001).
[9] G. Chen and W. A. Goddard III, Science **239**, 899 (1988)
[10] J. Casanovas, J. Rubio, and F. Illas, Phys. Rev. B **53**, 945 (1996).
[11] I. de P. R. Moreira, F. Illas, C. J. Calzado, J. F. Sanz, J. P. Malrieu, N. B. Amor, and D. Maynau, Phys. Rev. B **59**, R6593 (1999).
[12] D. Muñoz, F. Illas, and I. de P. R. Moreira, Phys. Rev. Lett. **84**, 1579 (2000).
[13] D. Muñoz, I. de P. R. Moreira, and F. Illas, Phys. Rev. B **65**, 224521 (2002).
[14] R. L. Martin and F. Illas, Phys. Rev. Lett. **79**, 1539 (1997).
[15] P. Rivero, I. de P. R. Moreira, and F. Illas, Phys. Rev. B **81**, 205123 (2010).
[16] F. C. Zhang and T. M. Rice, Phys. Rev. B **37**, 3759 (1988).
[17] P. W. Anderson, Science **235**, 1196 (1987).
[18] V. J. Emery, Phys. Rev. Lett. **58**, 2794 (1987).
[19] G. Baskaran, Mod. Phys. Lett. B **14**, 377 (2000).
[20] E. Pavarini, I. Dasgupta, T. Saha-Dasgupta, O. Jepsen, and O. K. Andersen, Phys. Rev. Lett. **87**, 047003 (2001).
[21] H. Eisaki, N. Kaneko, D. L. Feng, A. Damascelli, P. K. Mang, K. M. Shen, Z. X. Shen, and M. Greven, Phys. Rev. B **69**, 064512 (2004).
[22] V. I. Anisimov, M. A. Korotin, A. S. Mylnikova, A. V. Kozhevnikov, Dm. M. Korotin, and J. Lorenzana, Phys. Rev. B **70**, 172501 (2004).

[23]V. I. Anisimov, M. A. Korotin, I. A. Nekrasov, Z. V. Pchelkina, and S. Sorella, Phys. Rev. B **66**, 100502 (2002).
[24]C. H. Patterson, Phys. Rev. B **77**, 094523 (2008).
[25]V. I. Anisimov, F. Aryasetiawan, and A. I. Lichtenstein, J. Phys.: Condens. Matter **9**, 767 (1997).
[26]V. I. Anisimov, I. V. Solovyev, M. A. Korotin, M. T. Czyzyk, and G. A. Sawatzky, Phys. Rev. B **48**, 16929 (1993).
[27]I. V. Solovyev, P. H. Dederichs, and V. I. Anisimov, Phys. Rev. B **50**, 16861 (1994).
[28]A. D. Becke, J. Chem. Phys. **98**, 5648 (1993).
[29]C. Lee, W. Yang, and R.G. Parr, Phys. Rev. B **37**, 785 (1988).
[30]L. Hozoi, S. Nishimoto, G. Kalosakas, D. B. Bodea, and S. Burdin, Phys. Rev. B **75**, 024517 (2007).
[31]F. Ronning, C. Kim, D. L. Feng, D. S. Marshall, A. G. Loeser, L. L. Miller, J. N. Eckstein, I. Bozovic, and Z.-X. Shen, Science **282**, 2067 (1998).
[32]F. Ronning *et al.*, Phys. Rev. B **67**, 165101 (2003).
[33]T. Hanaguri, C. Lupien, Y. Kohsaka, D.-H. Lee, M. Azuma, M. Takano, H. Takagi, and J. C. Davis, Nature **430**, 1001 (2004).
[34]Y. Kohsaka, C. Taylor, K. Fujita, A. Schmidt, C. Lupien, T. Hanaguri, M. Azuma, M. Takano, H. Eisaki, H. Takagi, S. Uchid, and J. C. Davis, Science **315**, 1380 (2007).
[35]Y. Kohsaka, K. Iwaya, S. Satow, T. Hanaguri, M. Azuma, M. Takano, and H. Takagi, Phys. Rev. Lett. **93**, 097004 (2004).
[36]T. Hanaguri, Y. Kohsaka, J. C. Davis, C. Lupien, I. Yamada, M. Azuma, M. Takano, K. Ohishi, M. Ono, and H. Takagi, Nature Physics **3**, 865 (2007).
[37]T. Hanaguri, C. Lupien, Y. Kohsaka, D. H. Lee, M. Azuma, M. Takano, H. Takagi, and J. C. Davis, Nature **430**, 1001 (2004).
[38]Y. Kohsaka, C. Taylor, K. Fujita, A. Schmidt, C. Lupien, T. Hanaguri, M. Azuma, M. Takano, H. Eisaki, H. Takagi, S. Uchid, and J. C. Davis, Science **315**, 1380 (2007).
[39]Z. Hiroi, N. Kobayasi, and M. Takano, Physica C **266**, 191 (1996).
[40]D. N. Argyriou, J. D. Jorgensen, R. L. Hitterman, Z. Hiroi, N. Kobayashi, and M. Takano, Phys. Rev. B **51**, 8434 (1995).
[41]D. Vaknin, L. L. Miller, and J. L. Zarestky, Phys. Rev. B **56**, 8351 (1997).
[42]D. Hechel and I. Felner, Physica C **235–240**, 1601 (1994).
[43]R. Grau-Crespo, S. Hamad, C. R. A. Catlow, and N. H. de Leeuw, J. Phys.: Condens. Matter **19**, 256201 (2007).
[44]P. E. Blöchl, Phys. Rev. B **50**, 17953 (1994).
[45]G. Kresse and D. Joubert, Phys. Rev. B **59**, 1758 (1999).
[46]P. Rivero, I. de P. R. Moreira, and F. Illas, Phys. Rev. B **81**, 205123 (2010).
[47]W. H. Press, B. P. Flannery, S. A. Teukolsky, and W. T. Vetterling, *Numerical Recipes* (Cambridge University Press, New York, 1986).
[48]G. Kresse and J. Hafner, Phys. Rev. B **47**, 558 (1993).
[49]G. Kresse and J. Furthmüller, Phys. Rev. B **54**, 11169 (1996).
[50]I. de P. R. Moreira and R. Dovesi, Int. J. Quantum Chem. **99**, 805 (2004).